ROFC-LF: Recursive Online Fountain Code With Limited Feedback for Underwater Acoustic Networks

Xiuxiu Liu, Xiujuan Du, Jiliang Zhang, *Senior Member, IEEE*, Duoliang Han, and Long Jin, *Senior Member, IEEE*

***Abstract*— Online fountain codes (OFCs) have many advantages, such as low overhead, online feedback and optimal encoding, due to the feedback of the instantaneous decoding state. This paper analyzes the characteristics of underwater acoustic networks (UANs) as well as the issues of existing OFCs applied in UANs. Aiming at these issues, two optimization objectives of OFCs are put forward for UANs. In addition, a recursive OFC with limited feedback (ROFC-LF) is presented for UANs. The ROFC-LF reduces the consumption of bandwidth and energy caused by the transmission of useless coding packets. Through limited feedback, the problem of low channel utilization in UANs with half-duplex communication is solved. Furthermore, a data transmission mechanism based on the ROFC-LF for UANs is presented. The theoretical analysis and simulation results show that the proposed transmission mechanism based on the ROFC-LF scheme outperforms the existing OFC schemes in terms of overhead, computational complexity, coding efficiency and energy consumption. Consequently, the ROFC-LF is suitable for UANs with constrained resources.**

***Index Terms*— ROFC-LF, UANs, overhead, feedback, coding efficiency, computational complexity, energy consumption.**

I. Introduction

RECENTLY, underwater acoustic networks (UANs) have received widespread attention due to their potential applications in environmental monitoring, resource investigation, disaster prevention, etc. [1]–[3]. UANs adopt acoustic communication, which is characterized by a high bit error on the order of $10^{-3} - 10^{-7}$, a long propagation delay of a few seconds, and a narrow bandwidth of kbps [4]–[6]. Compared with conventional radio frequency (RF) modems, the acoustic modems in UANs consume more energy [7]–[8]. Additionally, energy savings are one of primary considerations in UANs design, as the nodes are powered by batteries, which are difficult to recharge and replace in harsh underwater environments [7]–[9]. In addition, acoustic modems operate in half-duplex mode, and an incoming feedback packet leads to a receiving-sending collision at the node sending packets. Furthermore, data transmission in UANs suffers from the Doppler effect and multipath propagation. All these factors bring about great challenges for the reliable transmission of UANs [19].

A. Related Work

In recent years, some scholars have investigated reliable transmission based on digital fountain codes (DFCs) for UANs. In 1998, Byers and Luby proposed the concept of DFCs in [10], which are mainly used for data transmission in binary erase channels (BECs). In 2002, Luby proposed the first practical DFC, Luby Transform (LT) code, in [11]. To avoid producing encoded packets with a larger degree, Shokrollahi proposed the Raptor code in [12]. Subsequently, DFCs attracted the attention of scholars worldwide. Some scholars have found that the degree distribution function, feedback, and encoding and decoding algorithms of DFCs have a great effect on network performance [13]–[17]. In [18], Yildiz investigated the problem of maximizing the network lifetime of UANs based on DFCs, and the results showed that DFC-based forward error correction methods can prolong the network lifetime by at least 16% compared with methods based on automatic repeat requests (ARQs). In [7], Du *et al.* put forward a handshake-free medium access control protocol for UANs based on recursive LT code. In [19], Song presented an analytical framework for evaluating the communication performances of UANs through DFC-based ARQ transmissions and formulated a joint optimization problem to minimize the total cost. In [20], Simao *et al.* analyzed the energy consumption of multihop UANs based on DFCs and concluded that this transmission scheme can save up to 40% of the energy consumption compared with the case without DFCs and the optimized modulation order.

Manuscript received 8 September 2021; revised 6 March 2022 and 26 April 2022; accepted 17 May 2022. Date of publication 30 May 2022; date of current version 15 July 2022. This work was supported in part by the National Natural Science Foundation of China No.61962052, in part by the Innovation Team Foundation of Qinghai Office Science and Technology No.2020-ZJ-903 and in part by the Research Fund for the Chunhui Program of Ministry of Education of China. The associate editor coordinating the review of this article and approving it for publication was I. B. Djordjevic. *(Corresponding author: Xiujuan Du.)*

Xiuxiu Liu is with the College of Computer, Qinghai Normal University, Xining 810008, China, and also with the Academy of Plateau Science and Sustainability, Xining 810008, China (e-mail: 1154894860@qq.com).

Xiujuan Du is with the Qinghai Provincial Key Laboratory of IoT, College of Computer, Qinghai Normal University, Xining 810008, China, and also with the State Key Laboratory of Tibetan Intelligent Information Processing and Application, Academy of Plateau Science and Sustainability, Xining 810008, China (e-mail: dxj@qhnu.edu.cn).

Jiliang Zhang is with the Department of Electronic and Electrical Engineering, The University of Sheffield, Sheffield S1 4DT, U.K. (e-mail: jiliang.zhang@sheffield.ac.uk).

Duoliang Han is with the College of Computer, Qinghai Normal University, Xining 810008, China (e-mail: 2945219148@qq.com).

Long Jin is with the School of Information Science and Engineering, Lanzhou University, Lanzhou 730000, China, and also with the Academy of Plateau Science and Sustainability, Xining 810008, China (e-mail: jinlongsysu@foxmail.com).

Color versions of one or more figures in this article are available at https://doi.org/10.1109/TCOMM.2022.3178764.

Digital Object Identifier 10.1109/TCOMM.2022.3178764

Since the decoding process of DFCs without any feedback cannot be controlled or monitored by receivers, the DFCs with online properties have been widely studied by scholars in recent years. The Growth code is a representative DFC with online performance; the encoded packets are transmitted to its receiver with a dynamically changing degree distribution [21]. An online fountain code (OFC) with low overhead was proposed by Cassuto and Shokrollahi in [22]. The OFC has the optimal encoding strategy, which is obtained through a given instantaneous decoding state. The overhead of the OFC is lower than that of the Growth code. In [23], Huang *et al.* proposed a framework based on random graph theory to analyze the OFC and proposed the improved online fountain code (IOFC). In [24], Huang and Yi proposed selecting the original packets that had been encoded less frequently to decrease the number of connected components, and the overheads of coding and feedback were demonstrated to be significantly reduced. In [25], Zhao *et al.* improved the OFC by sending some encoded packets with degree 1 prior to the build-up phase to increase the recovery rate in decoding. In [26], Cai *et al.* analyzed the impact of limited feedback and proposed two feedback point selection strategies. The experimental results showed that the OFC with partial feedback can achieve almost the same performance as the OFC with full feedback. In [27], to improve the intermediate decoding rate, Huang *et al.* presented two coding schemes called the online fountain code without build-up phase (OFCNB) and the systematic online fountain code (SOFC). Shi *et al.* investigated a new class of OFCs in [28]. The new OFC improves the intermediate recovery rate through a zigzag decodable online fountain (ZDOF) in the first phase and a buffer decoding method (BDM) in the second phase. The theoretical analysis and simulation results showed that the proposed scheme is superior to the conventional OFC. In [29], Huang *et al.* applied the OFC for wireless broadcast and proposed an improved broadcasting scheme. The simulation experiments showed that the proposed broadcast scheme has better performance than other broadcast schemes based on DFCs.

B. Motivations

The OFC has a lower overhead and a better online feedback performance than other types of coding mechanisms, such as LT code and Growth code. In [22], it was shown that the LT code, Growth code, and OFC need 1400, 1500 and 1200 coded packets, respectively, to recover 1000 original packets. Furthermore, to recover the same number of original packets, the OFC needs far fewer feedback packets than the Growth code, so OFC is more applicable to UANs with half-duplex communication, long propagation delay, constrained energy and low data rate. For the OFC, the receiver calculates the optimal degree according to the decoding state and feeds it back to the sender. When the optimal degree changes, the receiver feeds back the updated optimal degree to the sender quickly. Consequently, the OFC may produce a number of feedback packets. However, a large number of feedback packets lead to packet collision, reduce the channel utilization and network throughput of UANs, and increase the end-to-end delay. In addition, with the OFC, the received useless encoded packets may be discarded at the receiver. For wired networks with sufficient energy and bandwidth resources, the receiver's behavior of discarding useless encoded packets has no effect on the network performance. However, for UANs with constrained energy and bandwidth, useless coding packets consume extra energy and channel bandwidth, which is another problem that needs to be solved in UANs.

In summary, the OFC has a lower overhead and a better online feedback performance than other types of coding mechanisms. However, considering the characteristics of UANs, such as half-duplex communication, long propagation delay, limited energy, low bandwidth, and high energy consumption, there are two problems that need to be solved when an OFC is applied to UANs. One is that each encoded packet received is expected to be helpful for recovering the original packets. The other is that only a small number of feedback packets are required to be sent back to the node. Therefore, in this paper, we improve the OFC and propose the recursive online fountain code with limited feedback (ROFC-LF), which is more suitable for UANs.

C. The Main Contributions

According to the motivations of this work, we propose the ROFC-LF for UANs. The ROFC-LF enhances the probability that each coding packet is helpful for recovering the original packets, limits the number of feedback packets, and reduces the extra consumption of bandwidth and energy caused by the transmission of useless coding packets. Through limited feedback, the problem of low channel utilization in UANs with half-duplex communication is solved. Furthermore, a data transmission mechanism based on the ROFC-LF for UANs is presented.

The main contributions of the paper are highlighted below.

1) We propose a systematic analysis scheme for OFC taking the narrow bandwidth, limited energy, and half-duplex communication of UANs into account. To enhance the system reliability while reducing feedback burden, we propose two critical optimization objectives for the system, i.e.,improving the probability of useful coding packets and reducing the number of feedback packets.
2) The ROFC-LF scheme is proposed to approach the two optimization objectives by improving the completion phase of the traditional OFC. The ROFC-LF scheme reduces the probability of useless encoded packets through recursively encoding and limits the number of feedback packets through a decoding progress threshold.
3) The number of encoded packets and overhead of the ROFC-LF are analyzed based on the random graph theory, and other performance such as feedback, computational complexity and encoding efficiency are also analyzed. The theoretical analysis shows that the ROFC-LF is suitable for UANs.
4) Combined with the characteristics of UANs, a reliable transmission mechanism for UANs based on the ROFC-LF is presented. Through simulation experiments, the ROFC-LF is demonstrated to be superior in terms of overhead, feedback, computational complexity, coding efficiency and energy consumption.

The rest of the paper is organized as follows: Section II analyzes the OFC through a systematic analysis scheme and proposes two critical optimization objectives combined with the characteristics of UANs. Section III presents the ROFC-LF. Section IV analyzes the ROFC-LF. Section V explores the transmission mechanism. Section VI conducts performance evaluation. Finally, section VII concludes the paper.

II. Analysis of the OFC Applied in UANs

In this section, the OFC is introduced firstly. Then the UANs are analyzed through the underwater channel model. In view of the characteristics of UANs, we provide a systematic analysis scheme for the OFC, in which the cycles in the connected component, the probability of useless encoded packets, and the feedback problem of OFC are investigated. Finally, we present two optimization objectives of OFCs for UANs.

A. OFC Overview

Whether with OFCs or DFCs, packets are encoded with exclusive-or (XOR) operations. DFCs are a kind of high-performance sparse code based on a bipartite graph. In comparison with the DFC, the OFC has low overhead, online feedback and optimal encoding strategies, which are obtained through instantaneous decoding states. The OFC is a new rate-free code, and the decoding graph of the OFC is represented by unipartite graphs.

The encoding and decoding procedures of the OFC can be divided into two phases: the build-up phase and the completion phase. In the build-up phase, the sender transmits encoded packets with degree 2 until a feedback packet is received. The receiver receives the encoded packets with degree 2 and updates the decoding graph G (i.e., by increasing edges) until the size of the largest component is $|D|$, $|D| = \beta_0 k$ $(0 < \beta_0 < 1)$. Then, the receiver sends a feedback packet to tell the sender that the largest component has been built up. To decode the largest component, encoded packets with degree 1 need to be sent successively until the original packets in the largest component are recovered successfully.

In the completion phase, the receiver calculates the optimal degree according to the instantaneous decoding state, which is obtained by the receiver's decoding graph, and then feeds the optimal degree back to the sender. The sender encodes packets according to the optimal degree until all the original packets are recovered successfully. If the encoded packets fall into either Case 1 or Case 2, the receiver receives and processes them and updates the decoding graph. Otherwise, the encoded packets are useless and discarded.

Case 1: The received encoded packet is generated by XORing one original packet that has not been recovered and $m_{\text{opt}} - 1$ original packets that have been recovered.

Case 2: The received encoded packet is generated by XORing two original packets that have not been decoded and $m_{\text{opt}} - 2$ original packets that have been decoded successfully.

According to [22], the optimal degree m_{opt} is given by

$$m_{\text{opt}} = \arg\max_{m}[P_1(m,\beta) + P_2(m,\beta)]. \tag{1}$$

$P_1(m,\beta)$ and $P_2(m,\beta)$ are the probabilities of Case 1 and Case 2, respectively. The calculation formulas of

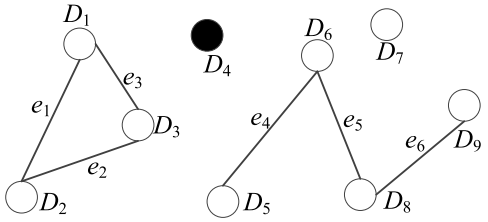

Fig. 1. The unipartite graph of the OFC.

$P_1(m,\beta)$ and $P_2(m,\beta)$ are

$$P_1(m,\beta) = \binom{m}{1}\beta^{m-1}(1-\beta). \tag{2}$$

$$P_2(m,\beta) = \binom{m}{2}\beta^{m-2}(1-\beta)^2. \tag{3}$$

The decoding graph of the OFC is represented by unipartite graphs. In a unipartite graph, a white vertex represents an original packet, and an edge between two white vertexes is used to represent an encoded packet generated by XORing the two corresponding original packets. A vertex is colored black if the original packet was recovered at the receiver (and white otherwise). The unipartite graph of the OFC with nine original packets is illustrated in Fig. 1. As shown in Fig. 1, vertex D_4 is black since the original packet D_4 has been recovered. The others vertexes are white. Edge $e_1(D_1, D_2)$ represents the encoded packet generated by XORing D_1 and D_2.

As shown in Fig. 1, the connected components are $\{D_1, D_2, D_3\}$, $\{D_5, D_6, D_8, D_9\}$ and $\{D_7\}$. The size of the maximum component is 4. The component $\{D_1, D_2, D_3\}$ is a cycle. We can obtain $D_1 + D_3$ by XORing $D_1 + D_2$ and $D_2 + D_3$; thus, the encoded packet $D_1 + D_3$ is redundant. Therefore, a cycle in a component implies redundant encoding.

B. The Features of UANs

UANs resort to acoustic communication. The propagation of acoustic signal is affected by the undulation of the sea surface, the uneven layering of the seabed, and the ambient noise. The non-uniformity of the seawater medium can cause scattering and refraction of acoustic wave. Therefore, the underwater acoustic channel is one of the most complex wireless channel. We first introduce the underwater channel model applied in this paper. Then, we analyze the characteristics of UANs.

1) Underwater Acoustic Channel Model: The signal attenuation in an underwater acoustic channel, denoted as $A(d,f)$, is a function of both distance d and frequency f. Then, for each hop, the attenuation $A(d,f)$, in dB, is given by [20]

$$10\log_{10}\frac{A(d,f)}{A_0} = 10\kappa\log_{10}d + \frac{d}{100}\log_{10}a(f). \tag{4}$$

where A_0 is a unit-normalizing factor, $10\kappa\log_{10}d$ is the spreading loss, d is the distance per hop in meters, and κ is a factor related to the geometry of propagation. $\frac{d}{100}\log_{10}a(f)$ is the absorption loss, and f is the frequency in kHz. $a(f)$ is the absorption coefficient in dB/km according to [20].

$$10\log_{10}a(f) = \frac{0.11f^2}{1+f^2} + \frac{44f^2}{4100+f^2} + 2.75\cdot 10^{-4}f^2 + 0.003. \tag{5}$$

Ambient noise for UANs consists of turbulence, shipping, waves, and thermal noise whose power spectral density (p.s.d.) in dB re μ Pa per Hz are represented by $N_t(f)$, $N_s(f)$, $N_w(f)$ and $N_{th}(f)$, respectively. The p.s.d. of the ambient noise $N(f)$ is given by [19]

$$N(f) = N_t(f) + N_s(f) + N_w(f) + N_{th}(f). \tag{6}$$

where $N_t(f)$, $N_s(f)$, $N_w(f)$ and $N_{th}(f)$ are four functions of f in kHz according to [19].

$$10\log_{10}N_t(f) = 17 - 30\log_{10}f, \tag{7}$$

$$10\log_{10}N_s(f) = 40 + 20(v - 0.5) + 26\log_{10}f - 60\log_{10}(f + 0.03), \tag{8}$$

$$10\log_{10}N_w(f) = 50 + 7.5w^{1/2} + 20\log_{10}f - 40\log_{10}(f + 0.4), \tag{9}$$

$$10\log_{10}N_{th}(f) = -15 + 20\log_{10}f, \tag{10}$$

where v is the movement factor of shipping with value-range from 0 to 1, and w is the speed of wind in m/s.

We approximate the p.s.d. of the ambient noise as [20]:

$$10\log_{10}N(f) \approx N_1 - \eta\log_{10}f. \tag{11}$$

where $N_1 = 50$ dB re μ Pa and $\eta = 18$ dB/decade.

Combining the attenuation and the p.s.d. of ambient noise, the average signal-to-noise ratio (SNR) for each hop is given by [20]

$$\bar{\gamma}(d, f) = \frac{p_{tx}}{A(d, f)N(f)M_dB}. \tag{12}$$

where p_{tx} is the transmitting power, M_d is the link margin and B is the channel bandwidth.

The instantaneous SNR is given by [20]

$$\gamma(d, f) = |h|^2\,\bar{\gamma}(d, f). \tag{13}$$

where h denotes the underwater acoustic channel fading.

2) The Characteristics of UANs: According to the underwater channel model, we can have: (i) The absorption coefficient increases rapidly as the frequency increases. At the same time, the attenuation also increases with the increase of propagation distance and frequency. Therefore, the available bandwidth of the underwater acoustic channel is limited. (ii) The attenuation, the ambient noise and the channel fading lower the SNR on the acoustic channel, resulting in high bit error rate in UANs.

In addition, acoustic communication results in long propagation delay in UANs. Each underwater sensor node is equipped with an acoustic modem, compared with conventional radio frequency (RF) modems, the acoustic modems in UANs consume more energy. However, the nodes are powered by batteries, which are difficult to recharge and replace in harsh underwater environments. Acoustic modems operate in half-duplex mode, an incoming feedback packet leads to a receiving-sending collision at the node sending packets. Therefore, UANs are characterized by high bit error, long propagation delay, narrow bandwidth, limited energy, and half-duplex communication. Data transmission in UANs suffers from the Doppler effect and multipath propagation. All these features pose great challenges for the reliable transmission of UANs.

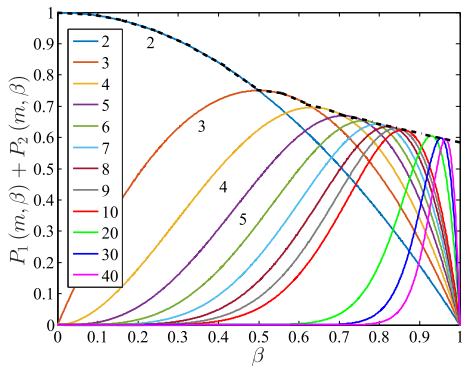

Fig. 2. $P_1(m, \beta) + P_2(m, \beta)$.

C. Analysis of the OFC Applied in UANs

The useless encoded packets in existing OFCs result in extra energy consumption and channel occupancy for UANs. A large amount of feedback causes packet collision, which decreases the channel efficiency and leads to a large end-to-end delay in UANs. In view of the characteristics of UANs, we propose a systematic analysis scheme for the OFC, which analyzes the cycles in the connected component, the probability of useless encoded packets, and the feedback problem of OFC.

1) Cycles: Fig. 1 shows that there is a cycle in one of the components. A cycle implies a redundant encoded packet. A redundant encoded packet is useless for decoding but consumes energy and channel bandwidth, which significantly reduces the performance of resource-constrained UANs. However, based on Lemmas 1 and 2, the appearance probability of cycles is very small, so the effect of useless encoded packets resulting from cycles can be neglected.

Lemma 1: The number of small components that have cycles is vanishingly small in the build-up phase [22][30].

Lemma 2: As the value of k goes to infinity, the probability that a cycle is introduced to a component by encoded packets in Case 2 is 0 in the completion phase [22].

2) Useless Encoded Packets: In addition to the useless encoded packets incurred by cycles, there are two other types of useless coding packets: one type results from duplicated encoded packets, and the other type is generated in the completion phase. These are neither Case 1 nor Case 2 types. It is easy to prove that the probability of generating duplicate encoding packets is very small. Therefore, we analyze useless encoded packets falling into the third type.

Fig. 2 shows the relationship between $P_1(m, \beta)+P_2(m, \beta)$ and β for different m with $k = 1000$. The maximum value of $P_1(m, \beta)+P_2(m, \beta)$ decreases with increasing β, as indicated by the dashed line in Fig. 2. The larger β is, the larger the optimal degree m_{opt} is. As decoding progresses, the probability of encoded packets falling into Case 1 or Case 2 decreases. Although the original packets are encoded with the optimal degree, there are still some useless encoded packets generated and sent in the OFC.

Theorem 1: In the completion phase, the upper bound on the probability of useless encoded packets p_{useless} is 0.4131.

Proof: The dashed line in Fig. 2 shows that the maximum value of $P_1(m, \beta) + P_2(m, \beta)$ decreases with increasing β. Therefore, when β is $(k - 1)/k$ (that is, only one original

packet is not successfully decoded.), $P_1(m_{\text{opt}},\beta)+P_2(m_{\text{opt}},\beta)$ should hit its minimal. However, when only one original packet is not successfully decoded, there is no encoded packet falling into Case 2. Thus, when β is $(k-1)/k$, the optimal degree m_{opt} is k. Then, the encoded packet is generated by XORing the unrecovered original packet and $k-1$ recovered original packets, and this encoded packet is of the Case 1 type. Therefore, when β is $(k-1)/k$, the probability that the generated encoded packet is a Case 1 type is 1; i.e., $P_{\beta=(k-1)/k}=1$.

When $\beta<(k-1)/k$, what is the probability that an encoded packet falls into Case 1 or Case 2? A theorem in [22] gives the answer as Lemma 3.

Lemma 3: For any β, there exists an m_{opt} such that

$$P_1(m_{\text{opt}},\beta)+P_2(m_{\text{opt}},\beta)>(1+\sqrt{2})e^{-\sqrt{2}}=0.5869. \tag{14}$$

where m_{opt} is the optimal degree among all m, with m and β satisfying formula (15).

$$\frac{\sqrt{(m-1)(m-2)}}{\sqrt{2}+\sqrt{(m-1)(m-2)}}\le\beta<\frac{\sqrt{m(m-1)}}{\sqrt{2}+\sqrt{m(m-1)}}. \tag{15}$$

Formula (15) is obtained by a formula in [22], which is

$$P_1(m,\beta)+P_2(m,\beta)=P_1(m+1,\beta)+P_2(m+1,\beta). \tag{16}$$

As seen in Fig. 2, there is an intersection point between two curves, one curve with degree m and another with degree $m+1$. The value of β at the intersection point is denoted by β_m, which can be calculated from formula (16).

Substituting $P_1(m,\beta)$ in (16) with equation (2) and $P_2(m,\beta)$ with equation (3), we obtain equation (17).

$$\beta_m=\frac{\sqrt{m(m-1)}}{\sqrt{2}+\sqrt{m(m-1)}}. \tag{17}$$

We substitute m in equation (17) with $m-1$ and obtain equation (18).

$$\beta_{m-1}=\frac{\sqrt{(m-1)(m-2)}}{\sqrt{2}+\sqrt{(m-1)(m-2)}}. \tag{18}$$

TABLE I lists the specific value range of β, i.e., $\left(\frac{\sqrt{(m-1)(m-2)}}{\sqrt{2}+\sqrt{(m-1)(m-2)}}\le\beta<\frac{\sqrt{m(m-1)}}{\sqrt{2}+\sqrt{m(m-1)}}\right)_{m=1}^{\infty}$.

We can easily obtain $\lim_{m\to\infty}\frac{\sqrt{m(m-1)}}{\sqrt{2}+\sqrt{m(m-1)}}=1$. In summary, $P_1(m_{\text{opt}},\beta)+P_2(m_{\text{opt}},\beta)>0.5869$ for any β. The probability sum of useless encoded packets p_{useless} and useful encoded packets falling into Case 1 or Case 2 is 1. Therefore, we obtain

$$p_{\text{useless}}=1-(P_1(m_{\text{opt}},\beta)+P_2(m_{\text{opt}},\beta))<0.4131. \tag{19}$$

We have now proved that in the completion phase, the upper bound on the probability of useless encoded packets p_{useless} is 0.4131. ■

According to Theorem 1, the larger β is, the larger p_{useless} is (except for $b=(k-1)/k$). Although the OFC is encoded with the optimal degree, some useless encoded packets are still generated. UANs have the characteristics of low data rate and limited energy. These useless encoding packets consume extra energy and channel bandwidth, shortening the lifetime of UANs. Therefore, in UANs, all the encoded packets are expected to be helpful for recovering the original packets.

TABLE I
THE RANGE OF β AND THE CORRESPONDING m VALUES

β	m	β	m	β	m
[0,0.5)	2	[0.8812,0.8904)	12	[0.9354,0.9383)	22
[0.5,0.634)	3	[0.8904,0.8983)	13	[0.9383,0.9408)	23
[0.634,0.7101)	4	[0.8983,0.9051)	14	[0.9408,0.9432)	24
[0.7101,0.7597)	5	[0.9051,0.9111)	15	[0.9432,0.9454)	25
[0.7597,0.7948)	6	[0.9111,0.9163)	16	[0.9454,0.9474)	26
[0.7948,0.8209)	7	[0.9163,0.9210)	17	[0.9474,0.9493)	27
[0.8209,0.8411)	8	[0.9210,0.9252)	18	[0.9493,0.9511)	28
[0.8411,0.8571)	9	[0.9252,0.9290)	19	[0.9511,0.9527)	29
[0.8571,0.8703)	10	[0.9290,0.9324)	20	[0.9527,0.9542)	30
[0.8703,0.8812)	11	[0.9324,0.9354)	21	···	···

3) Feedback Packets: Theorem 2: When $m_{\text{opt}}\in[15,k]$, the values of β_m and β are greater than 0.9, which means that fewer than $0.1k$ original packets are unrecovered at this moment according to the definitions of β and β_m. m_{opt} changes more frequently with the increasing of β. To feed the frequently changing m_{opt} back to the receiver, the receiver has to frequently send feedback packets.

Proof: Fig. 3 shows the relationship between β_m and m according to formula (17). According to formula (15) and TABLE I, one m value corresponds to a β_m and a certain range of β. When $m_{\text{opt}}=15$, $\beta_m=0.9111$, and $\beta\in[0.9051,0.9111)$, it is seen from TABLE I that with increasing β, m_{opt} increases rapidly. When $m_{\text{opt}}=15$, the value of β is greater than 0.9. Thus, we can easily conclude that fewer than $0.1k$ original packets are unrecovered when $m_{\text{opt}}\ge 15$; however, when m_{opt} changes more frequently, to feed the frequently changed m_{opt} back to the receiver, the receiver must send frequent feedback packets. ■

Theorem 3: With the increasing of m_{opt}, the value-range of β corresponding to m_{opt} decreases and tends toward 0. Therefore, as decoding progresses, m_{opt} changes more quickly, and more feedback packets are needed.

Proof: It can be seen from TABLE I that when β is in the range (0,0.5], the optimal degree m_{opt} is 2; when β is in the range (0.5,0.634], the optimal degree m_{opt} is 3; and when β is in the range (0.6340,0.7101], the optimal degree m_{opt} is 4. From equations (17) and (18), we obtain equation (20).

$$\begin{aligned}\Delta\beta_s&=\beta_m-\beta_{m-1}\\&=\frac{\sqrt{m(m-1)}}{\sqrt{2}+\sqrt{m(m-1)}}-\frac{\sqrt{(m-1)(m-2)}}{\sqrt{2}+\sqrt{(m-1)(m-2)}}.\end{aligned} \tag{20}$$

According to equation (20), we calculate the value of $\Delta\beta_s$, as shown in TABLE II. As seen from TABLE II, with increasing β, $\Delta\beta_s$ decreases. The smaller $\Delta\beta_s$ is, the more frequently m_{opt} changes, and thus, the more feedback packets are needed. By calculating the limit of $\Delta\beta_s$, the following results are obtained: with increasing m_{opt}, the interval of β corresponding to m_{opt} decreases and tends toward 0. Therefore, as decoding progresses, m_{opt} changes more quickly, and more feedback

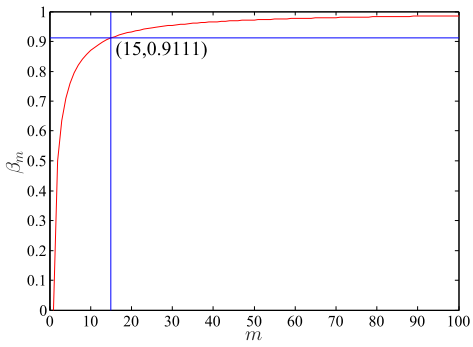

Fig. 3. Relationship between β_m and m.

TABLE II
$\Delta\beta_s$ AND THE CORRESPONDING m_{OPT} VALUES

$\Delta\beta_s$	m_{opt}	$\Delta\beta_s$	m_{opt}	$\Delta\beta_s$	m_{opt}	$\Delta\beta_s$	m_{opt}
0.5	2	0.0132	10	0.0042	18	0.002	26
0.134	3	0.0109	11	0.0038	19	0.0019	27
0.0761	4	0.0092	12	0.0034	20	0.0018	28
0.0496	5	0.0079	13	0.003	21	0.0016	29
0.0351	6	0.0068	14	0.0029	22	0.0015	30
0.0261	7	0.006	15	0.0025	23	...	...
0.0202	8	0.0052	16	0.0024	24	...	...
0.016	9	0.0047	17	0.0022	25	...	...

packets are needed.

$$\lim_{m\to\infty} \Delta\beta_s = \lim_{m\to\infty} \frac{\sqrt{m(m-1)}}{\sqrt{2}+\sqrt{m(m-1)}} - \frac{\sqrt{(m-1)(m-2)}}{\sqrt{2}+\sqrt{(m-1)(m-2)}} = 0. \quad (21)$$

■

Through the above analyses, we can conclude that when the OFC is directly applied to UANs, there are two fatal disadvantages. One is that when fewer than $0.1k$ original packets are unrecovered, to feed the constantly changing m_{opt} back in a timely manner, the receiver has to send many feedback packets to the sender. The other is that as decoding progresses, the feedback becomes increasingly frequent, which leads to packet collision and frequent switching between the receiving and sending states of underwater modems, prolongs the end-to-end delay and consumes much energy. Therefore, when the OFC is applied to UANs, the issue of frequent feedback should be addressed.

D. The Optimization Objective of the OFC for UANs

The network model of a UAN is shown in Fig. 4. Data packets are transmitted along the paths from the respective source nodes (underwater sensor nodes) to the sink node through multiple hops. Each underwater sensor node is equipped with an acoustic modem, which operates in half-duplex mode. The sink node is equipped with an acoustic modem that communicates with underwater nodes and an RF modem that communicates with terrestrial base stations. The underwater acoustic channel is considered a quasi-static fading channel. For the sake of simplicity, we assume that the used underwater

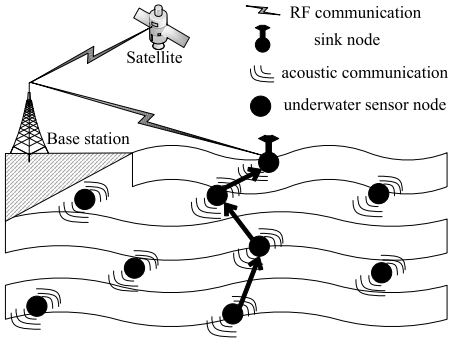

Fig. 4. Network model.

channel is known by the sender and receiver. Compared with conventional RF modems, acoustic modems in UANs consume more energy. Switching the state of an acoustic modem from receiving to transmitting or from transmitting to receiving requires a long delay.

In each hop, a sender encodes the original data packets and sends the encoded packets to the next-hop node, and the receiver recovers the original packets through decoding and then reencodes the original packets and forwards the reencoded packets to the next-hop node along the path.

Through the detailed analysis in section II.C, we found that (i) the probability of forming cycles in the connected components in the build-up phase is very small, and the useless encoded packets resulting from cycles can be ignored. (ii) Although the original data packets are encoded by the optimal strategy in the completion phase of the OFC, some encoded packets that are useless for decoding are still generated and transmitted. (iii) Due to the optimal strategy, the number of feedback packets with the OFC is less than that with the Growth code. However, as decoding progresses, the feedback becomes increasingly frequent. Considering the characteristics of UANs, the transmission of useless encoded packets wastes channel bandwidth and increases delay and energy consumption. Excessive feedback packets will lead to packet collision and frequent state switching of underwater modems between receiving and sending. All these factors cause long delay, extra energy consumption, and low channel utilization in UANs. To design an OFC that consumes less bandwidth and energy than state-of-the-art OFC in bandwidth-constrained and energy-constrained UANs, we present two optimization objectives of OFCs for UANs: the first is to improve the probability of useful coding packets, and the second is to decrease the number of feedback packets.

III. ROFC AND ROFC-LF CODINGS

A. The ROFC Mechanism

To decrease energy consumption and improve channel efficiency in UANs, all the encoded packets are expected to be helpful for recovering the original packets. In accordance with the characteristics of UANs, based on the first optimization objective of OFCs, this paper proposes the recursive online fountain code (ROFC) for UANs. With the ROFC, the original packets are classified into two sets, the recovered set and unrecovered set. The encoded packets are generated by XORing

the original packets in the unrecovered set, so each encoded packet is helpful for decoding.

In addition, to reduce the size of the feedback packets, the states and the serial numbers (SNs) of the original packets are encoded and fed back to the sender as given in the recursively encoding strategy.

1) The Recursively Encoding Strategy: The receiver encodes the SNs of all the original packets and feeds back the encoded SNs and the corresponding states to the sender. Then, the sender encodes recursively so that all the encoded packets are useful for the decoding process in the completion phase, which decreases energy consumption and improves channel efficiency in UANs.

According to the decoded graph G, the decoding state can be represented by formula (22).

$$F(A) = \bigcup_{j=1}^{|A|} SN_j. \tag{22}$$

where A is a set of $|A|$ black vertexes and SN_j represents the SN of a black vertex.

If the feedback packet contains the unencoded SNs and the states of the original packets, the size of the feedback packet will be very long, which will consume much energy in the UAN. Therefore, to reduce the length of the feedback packet, the SNs and the states of the original packets are encoded as described below.

In the feedback packet, there are k bits in the state field, one bit for each original packet. The value of the kth bit indicates the state of the kth original packet, which is represented by 0 or 1. The "0" in the sixth bit indicates that the sixth original packet has not been recovered, and the "1" in the third bit indicates that the third original packet has been recovered successfully. When there are $|A|$ black vertexes, $|A|$ bits in the state field are set to 1, and $k - |A|$ bits are set to 0. Suppose k is 10 and the instantaneous decoding state is $F(3) = \{1, 4, 7\}$. Then, the encoded state field is expressed as $F'(3) = \{1, 0, 0, 1, 0, 0, 1, 0, 0, 0\}$. Therefore, the state field of a feedback packet is given by

$$F'(A) = \left\{ \overbrace{\underbrace{0,0,0,0\ldots,1,0,0\ldots,0,1,0}}^{k \text{ bits, the number of 1 is } |A|} \right\}. \tag{23}$$

Considering the case in which the SNs are not encoded, suppose there are 1000 original packets (i.e., $k = 1000$) and the SN of each original packet accounts for at least 10 bits. If 560 original packets have been successfully recovered and the SN field is directly filled in the feedback packet, the length of the SN field in the feedback packet will be 560*10 bits. If the SNs are encoded, then the length of the state field is 1000 bits, and the length of a feedback packet is greatly reduced by encoding the SNs, which is preferable for resource-constrained UANs.

Based on the state field of the feedback packets, the sender divides the original packets into two sets. One set contains the recovered original packets, denoted as $Y_i(|A|, SNs)$. The other set contains the original packets that have not been recovered, denoted as $W_i(k - |A|, SNs)$. After the sender receives a feedback packet, the value of i increases by 1, and the two sets $Y_i(|A|, SNs)$ and $W_i(k-|A|, SNs)$ are updated. Based on the set $W_i(k - |A|, SNs)$ and our recursive coding scheme, we define the following two cases:

Case 1: Randomly select an original packet from the set $W_i(k - |A|, SNs)$ to generate an encoded packet with degree 1.

Case 2: Randomly select two original packets from the set $W_i(k - |A|, SNs)$ to generate an encoded packet with degree 2.

The probability of an encoded packet falling into Case 1 is α, and the probability of it falling into Case 2 is θ. If the upper bound on the degree of an encoding packet is "2," then α and θ satisfy the following expression:

$$\alpha + \theta = 1. \tag{24}$$

B. The ROFC-LF Mechanism

The ROFC is proposed according to the first optimization objective, which ensures that each encoded packet is useful for recovering the original packets. According to the second optimization objective, the number of feedback packets must be restricted while ensuring the optimal coding strategy. Therefore, we propose the ROFC-LF for UANs, which reduces the number of feedback packets. To construct the ROFC-LF, the feedback strategy is given as follows:

1) The Feedback Strategy: The feedback is restricted by setting the threshold of $\Delta\beta$. $\Delta\beta$ is the difference in β; i.e., $\Delta\beta = \beta_{t_2} - \beta_{t_1} (t_2 > t_1)$.

The threshold of $\Delta\beta$ is set to δ. According to Theorems 2 and 3, as decoding progresses, $\Delta\beta_s$ decreases, which leads to frequent feedback. Referring to Fig. 3, when β is greater than 0.9111, less than $0.1k$ original packets are not recovered. To reduce the negative effect of too much feedback on the UAN, the feedback needs to be restricted by setting a threshold of $\Delta\beta$. We first set $\delta = 0.006$.

In the completion phase of the ROFC-LF, the receiver encodes the SNs of all original packets and feeds back the states of the original packets to the sender. According to the threshold δ, the receiver determines whether to send a feedback packet. Then, the original packets are classified into two sets by the sender: the recovered set $Y_i(|A|, SNs)$ and unrecovered set $W_i(k - |A|, SNs)$. The encoded packets, either in Case 1 or Case 2, are generated recursively by XORing the original packets in the unrecovered set. The encoding and decoding process continues in this way until all original packets are recovered successfully.

C. Encoding and Decoding

The proposed ROFC scheme does not limit the number of feedback packets. As long as $\Delta\beta > 0$, the receiver with the ROFC sends a feedback packet. However, only when $\Delta\beta > \delta$ does the receiver with the ROFC-LF send a feedback packet. Otherwise, the encoding and decoding processes of the ROFC and ROFC-LF are the same. The encoding and decoding processes of the ROFC and ROFC-LF are also divided into two phases: the build-up phase and the completion phase. Suppose the sender has k original packets to transmit. The detailed encoding and decoding processes are described below.

1) Encoding: In the build-up phase, the sender generates and sends encoded packets with degree 2 until the size of the largest connected component is $|D| = \beta_0 k$ $(0 < \beta_0 < 1)$; then, it starts to transmit packets with degree 1 until the original packets in the largest component are recovered successfully.

In the completion phase, according to the states of the original packets in the feedback packets, the original packets are classified into two sets, $Y_i(|A|, SNs)$ and $W_i(k-|A|, SNs)$. After receiving a feedback packet, the receiver adds 1 to i and updates the two sets $Y_i(|A|, SNs)$ and $W_i(k-|A|, SNs)$. Then, the sender generates and sends the encoded packets with only degree 1 or degree 2 according to Case 1 or Case 2 as in section III.A. The original packets in $W_i(k-|A|, SNs)$ are encoded in this way until they are all decoded successfully.

2) Decoding: Initially, the receiver maintains a decoding graph $G = (V, E)$ with k white nodes and no edges, where $|V| = k$ and $E = \emptyset$.

In the build-up phase, the sender generates and transmits encoded packets with degree 2. After receiving an encoded packet with degree 2, the receiver updates the decoding graph G by adding an edge. When the size of the largest component reaches $\beta_0 k$, the receiver sends the feedback packet to tell the sender that the packets with degree 1 need to be sent next. After receiving a packet with degree 1, the receiver colors the original packet black and then XORs the original packet with other related encoded packets in a component to decode them continually. When all the original packets in the largest component are black, the build-up phase ends, and the receiver sends the feedback packet, including the states of all the original packets, to the sender.

In the completion phase of the ROFC-LF, the sender transmits only encoded packets with degree 1 or 2. The receiver recovers the original packets by decoding, updates the decoding graph G, and calculates $\Delta\beta$. According to the threshold δ, the receiver determines whether to send a feedback packet. The encoding and decoding process continues in this way until all original packets are decoded successfully.

IV. Analysis of the ROFC-LF

The data packets in UANs are transmitted from the source node to the sink node through multiple hops, and the mechanism of encoding and decoding is the same in each hop. This section analyzes the number of encoded packets and feedback packets required to recover k original packets for a single hop as well as the overhead, computational complexity, and encoding and decoding efficiency of the ROFC-LF based on random graph theory. When the proposed ROFC-LF scheme does not limit feedback (i.e., $\delta = 0$), it is indicated as ROFC. The four coding schemes ROFC-LF, ROFC, OFC(the online fountain code in [22]) and IOFC(the improved online fountain code in [23]) are analyzed.

A. Analysis of Codecs

In this section, we analyze how many encoded packets are transmitted to recover the k original packets in single-hop transmission in a UAN. The proposed ROFC scheme does not limit the number of feedback packets; as long as $\Delta\beta > 0$, the receiver with the ROFC sends a feedback packet. With the ROFC, all the encoded packets are expected to be helpful for recovering the original packets. However, the proposed ROFC-LF scheme limits the number of feedback packets, which may result in useless encoded packets being generated and transmitted in the completion phase. Here, we first analyze the ROFC.

In the build-up phase, the ROFC scheme is the same as that of the OFC. As presented in [22], a random graph $g(k, p)$ is constructed by randomly adding edges in the build-up phase, where p is the probability that an edge is selected; $p = c/k$. c is the average number of times that a vertex is selected. A vertex is equivalent to an original packet. The random graph $g(k, p)$ has k vertexes and $k(k-1)/2$ edges at most [31, Ch 10]. Next, Lemma 4 is introduced to describe the relationship between c and β_0.

Lemma 4: The frequency c with which each original packet is selected and the fraction of the largest component β_0 satisfy the constraint

$$\beta_0 + \mathrm{e}^{-c\beta_0} = 1. \tag{25}$$

Lemma 5: In [23], the expected number of encoded packets with degree 2 $N_{d=2}$ at the end of the build-up phase is given by

$$N_{d=2} = kc/2, \tag{26}$$

and the expected number of encoded packets with degree 1 $N_{d=1}$ at the end of the build-up phase is given by

$$N_{d=1} = 1/\beta_0. \tag{27}$$

Theorem 4: In the completion phase, the expected number of encoded packets falling into Case 1 or Case 2 $N_{d=1|2}$ is

$$N_{d=1|2} = k(1-\beta_0)[1 - c(1-\beta_0)/2]. \tag{28}$$

Proof: According to [22], subgraph $g'(t, d)$ is a random graph identical to the random graph $g(k, p)$ except that the largest component $k\beta_0$ is removed at the beginning of the completion phase. t denotes the number of vertexes in the subgraph g', where $t = k(1-\beta_0)$. d denotes the frequency with which each original packet is selected, where $d = c(1-\beta_0)$. The t vertexes are selected to form edges, and the expected number of edges at the end of the build-up phase is

$$N_{g'} = td/2 = k(1-\beta_0)c(1-\beta_0)/2. \tag{29}$$

Lemma 6: On average, the recovery of one original packet in the completion phase requires one useful encoded packet to be transmitted [23].

The useful encoded packets in the ROFC fall into either Case 1 or Case 2. Considering the number of existing edges $N_{g'}$ at the end of the build-up phase, based on Lemma 6, the required number of useful encoded packets(i.e., packets in Case 1 or Case 2) that must be transmitted to recover t original packets is

$$N_t = t - N_{g'} = t - td/2. \tag{30}$$

In the encoding process, the duplicated encoded packets and the encoded packets connecting a component into a cycle are useless for recovering the original packets. Based

on Lemmas 1 and 2, there are very few cycles in the OFC. The ROFC also has very few cycles. Each time the receiver receives an encoded packet with degree 1, it sends a feedback packet to the sender. After receiving a feedback packet, the sender updates the set $W_i(k-|A|, SNs)$. Therefore, no duplicated encoded packet with degree 1 is transmitted. The probability of producing duplicated encoded packets with degree 2 in the ROFC is

$$P_s = \frac{2}{(k-k\beta_1)(k-k\beta_1-1)}. \tag{31}$$

where, according to the i-th feedback, the number of original packets that have been successfully decoded is $k\beta_1$; then, $|W_i(k-|A|, SNs)| = k-k\beta_1$. According to the j-th feedback ($j > i$), the number of original packets that have been successfully decoded is $k\beta_1 + \Delta\beta k$; then, $|W_j(k-|A|, SNs)| = k-k\beta_1-\Delta\beta k$.

Fig. 5 is the simulation result of the curve of P_s versus β_1, in which $k = 1000$. When $k\beta_1 = 955$, $P_s = 0.001$. As in Fig. 5, when $\beta_1 \in (0, 0.955]$, $\lim_{\beta_1 \to 0.955} P_s = 0$. When $\beta_1 \in (0.955, 1]$, the probability P_s is greater than 0. Therefore, the probability of generating duplicated encoded packets with the ROFC is negligible.

In the completion phase of the ROFC, all the encoded packets fall into either Case 1 or Case 2. There are very few useless encoded packets, and they can be ignored. The total probability of Case 1 and Case 2 is $\alpha+\theta = 1$. Therefore, the expected number of encoded packets falling into Case 1 or Case 2, $N_{d=1|2}$, is

$$\begin{aligned} N_{d=1|2} &= (\alpha+\theta)\cdot N_t = N_t = t - td/2 \\ &= k(1-\beta_0)[1-c(1-\beta_0)/2]. \end{aligned} \tag{32}$$

■

Then, the number of Case 1 encoded packets is $N_{\text{Case 1}} = \alpha \cdot N_t$, and the number of Case 2 encoded packets is $N_{\text{Case 2}} = \theta \cdot N_t$. Therefore, combined with formulas (24) and (28), formulas (33) and (34) are obtained.

$$N_{\text{Case 1}} = \alpha \cdot k(1-\beta_0)[1-c(1-\beta_0)/2]. \tag{33}$$

$$N_{\text{Case 2}} = \theta \cdot k(1-\beta_0)[1-c(1-\beta_0)/2]. \tag{34}$$

Theorem 5: To recover all k original packets, the expected total number of encoded packets in the ROFC is

$$\begin{aligned} E(N)_{\text{ROFC}} &= N_{d=2} + N_{d=1} + N_{d=1|2} \\ &= kc/2 + 1/\beta_0 + k(1-\beta_0)[1-c(1-\beta_0)/2]. \end{aligned} \tag{35}$$

Proof: There are three types of encoded packets: the first type is encoded packets with degree 2 in the build-up phase, the second is encoded packets with degree 1 in the build-up phase, and the third is encoded packets falling into Case 1 or Case 2 in the completion phase. Therefore, to recover all k original packets, the total number of encoded packets required is the sum of the expected numbers of the three types of encoded packets. Then, combining Lemma 5 and Theorem 4, Theorem 5 is verified. ■

In the ROFC-LF, the frequency of feedback packets is restricted, and the set $W_i(k-|A|, SNs)$ is not updated in a timely manner. Thus, some useless encoded packets may be generated with the ROFC-LF. Therefore, to recover k original packets, the expected number of encoded packets transmitted with the ROFC-LF is

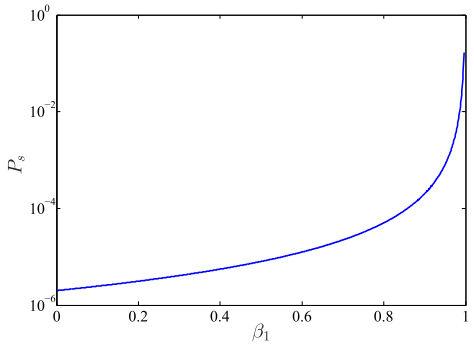

Fig. 5. Relationship between β_1 and P_s.

$$E(N)_{\text{ROFC - LF}} \geq \frac{kc}{2} + \frac{1}{\beta_0} + k(1-\beta_0)\left[1 - \frac{c(1-\beta_0)}{2}\right]. \tag{36}$$

According to [23], the expected numbers of encoded packets with the OFC and the IOFC are $E(N)_{\text{OFC}}$ and $E(N)_{\text{IOFC}}$, respectively.

$$\begin{aligned} E(N)_{\text{OFC}} = {} & \frac{kc}{2} + \frac{1}{\beta_0} + \left[1 - \frac{c(1-\beta_0)}{2}\right] \\ & \times \sum_{i=1}^{k-k\beta_0} \frac{1}{P_1(m_{\text{opt}}, \beta_0 + \frac{i}{k}) + P_2(m_{\text{opt}}, \beta_0 + \frac{i}{k})}. \end{aligned} \tag{37}$$

$$\begin{aligned} E(N)_{\text{IOFC}} = {} & \frac{k}{2} + \frac{kc}{4} + \frac{1}{\beta_0} + \left[\frac{1}{2} - \frac{c(1-\beta_0)}{4}\right] \\ & \times \sum_{i=1}^{k-k\beta_0} \frac{1}{P_1(m_{\text{opt}}, \beta_0 + \frac{i}{k}) + P_2(m_{\text{opt}}, \beta_0 + \frac{i}{k})}. \end{aligned} \tag{38}$$

B. Analysis of Feedback

The number of feedback packets is defined as N_{feedback}. In the build-up phase, when the size of the largest component reaches $\beta_0 k$ or the largest component is decoded successfully, the receiver sends a feedback packet, and then, $N_{\text{feedback}} = 2$ in the build-up phase. In the completion phase, whenever $\Delta\beta \geq \delta$ with the ROFC-LF or $\Delta\beta > 0$ with the ROFC, a feedback packet is transmitted, so $N_{\text{feedback}} = N_{\text{feedback}} + 1$.

For the ROFC, the number of feedback packets required is related to α or θ. If α is larger than θ, a large number of encoded packets with degree 1 are transmitted. Each encoded packet with degree 1 can result in one or more original packets being recovered. An encoded packet with degree 2 may connect two components into one component. Therefore, encoded packets with either degree 1 or degree 2 can lead to decoding progress, but they have different effects on feedback. When an encoded packet with degree 1 is received, one or more original packets can be recovered. The recovery of original packets results in an increase in β, so a feedback packet may be sent by the receiver. In contrast, an encoded packet with

degree 2 may merge two connected components, which does not trigger the feedback packet. Therefore, the larger α is, the more feedback packets are required. For UANs, a large number of feedback packets lead to packet collision, which decreases the channel utilization and increases the end-to-end delay; thus, a small α is preferable in UANs.

Corollary 1: With the ROFC, the number of feedback packets in the completion phase is equal to the number of encoded packets in Case 1; i.e., $N_{\text{feedback}} = N_{\text{Case 1}}$.

Proof: In the ROFC, when $\Delta\beta > 0$, a feedback packet is sent by the receiver. As long as an encoded packet falling into Case 1 is received, one or more original packets will be successfully decoded, and the value of β will increase, which results in $\Delta\beta > 0$. Then, a feedback packet is sent. Therefore, in the completion phase, the number of feedback packets is equal to the number of encoded packets falling into Case 1.■

Corollary 2: In the ROFC-LF, the number of feedback packets in the completion phase is less than or equal to the number of encoded packets in Case 1; i.e., $N_{\text{feedback}} \leq N_{\text{Case 1}}$.

Proof: If the receiver receives an encoded packet of Case 2 type, β remains unchanged; only when the receiver receives an encoded packet in Case 1 does β increase. Therefore, only an encoded packet of Case 1 type may cause $\Delta\beta \geq \delta$. When $\Delta\beta \geq \delta$, the receiver sends a feedback packet. Consequently, $N_{\text{feedback}} \leq N_{\text{Case 1}}$. ■

According to Corollary 1 and Corollary 2, the number of feedback packets required by the ROFC-LF is less than that required by the ROFC. According to the characteristics of UANs, the ROFC-LF is preferable for UANs.

C. Analysis of Overhead

Definition 1: When k original packets are recovered, the ratio of the number of redundant encoded packets (the total number of encoded packets minus k) to k is defined as the overhead, denoted by p_{oh}.

$$p_{\text{oh}} = \frac{N_{\text{total}} - k}{k}. \tag{39}$$

where N_{total} is the total number of encoded packets transmitted when k original packets are recovered.

In this paper, the overheads of the ROFC, ROFC-LF, OFC and IOFC are defined as $p_{\text{oh}}^{\text{ROFC}}$, $p_{\text{oh}}^{\text{ROFC - LF}}$, $p_{\text{oh}}^{\text{OFC}}$ and $p_{\text{oh}}^{\text{IOFC}}$, respectively. Based on the above analysis and formulas (35), (36), (37) and (38), we can obtain the overheads of the four coding schemes, which are given by the four formulas below. For resource-constrained UANs, the smaller the overhead is, the better.

$$p_{\text{oh}}^{\text{ROFC}} = \frac{E(N)_{\text{ROFC}} - k}{k} = \frac{1}{k\beta_0} - \frac{c\beta_0^2}{2} + c\beta_0 - \beta_0. \tag{40}$$

$$\begin{aligned} p_{oh}^{ROFC-LF} &= \frac{E(N)_{ROFC-LF} - k}{k} \\ &\geq \frac{1}{k\beta_0} - \frac{c\beta_0^2}{2} + c\beta_0 - \beta_0. \end{aligned} \tag{41}$$

$$\begin{aligned} p_{\text{oh}}^{\text{OFC}} &= \frac{E(N)_{\text{OFC}} - k}{k} \\ &= \frac{c}{2} + \frac{1}{k\beta_0} + \left[\frac{1}{k} - \frac{c(1-\beta_0)}{2k}\right] \\ &\quad \times \sum_{i=1}^{k-k\beta_0} \frac{1}{P_1(m_{\text{opt}}, \beta_0 + \frac{i}{k}) + P_2(m_{\text{opt}}, \beta_0 + \frac{i}{k})} - 1. \end{aligned} \tag{42}$$

$$\begin{aligned} p_{\text{oh}}^{\text{IOFC}} &= \frac{E(N)_{\text{IOFC}} - k}{k} \\ &= \frac{c}{4} + \frac{1}{k\beta_0} + \left[\frac{1}{2k} - \frac{c(1-\beta_0)}{4k}\right] \\ &\quad \times \sum_{i=1}^{k-k\beta_0} \frac{1}{P_1(m_{opt}, \beta_0 + \frac{i}{k}) + P_2(m_{opt}, \beta_0 + \frac{i}{k})} - \frac{1}{2}. \end{aligned} \tag{43}$$

D. Analysis of Computational Complexity

The computational complexities of the four encoding mechanisms ROFC, ROFC-LF, OFC and IOFC are defined as the respective numbers of XOR operations for encoding and decoding. In the build-up phase, with any one of the four coding schemes, only encoded packets with degree 2 or degree 1 are transmitted. In the completion phase, with either the OFC or the IOFC, encoded packets with degree m may be transmitted. However, with the ROFC (or the ROFC-LF), only encoded packets with degree 1 or degree 2 are generated and transmitted in the completion phase. An encoded packet with degree 1 is generated without XOR operations. An encoded packet with degree 2 is generated by performing one XOR operation. An encoded packet with degree m is generated by performing $m-1$ XOR operations. Based on the above analysis and formulas (35), (36), (37) and (38), we can obtain the computational complexities of the four coding schemes, which are given by the four formulas below. When β_0 is determined, the computational complexities of the proposed ROFC and ROFC-LF are both $O(k)$. However, the computational complexities of the OFC and IOFC are related to k and m.

$$O_{\text{ROFC}} = kc + 2\theta k(1-\beta_0)[1 - c(1-\beta_0)/2]. \tag{44}$$

$$O_{\text{ROFC - LF}} \geq kc + 2\theta k(1-\beta_0)[1 - c(1-\beta_0)/2]. \tag{45}$$

$$\begin{aligned} \text{O}_{\text{OFC}} &= kc + 2(m-1)\left[1 - \frac{c(1-\beta_0)}{2}\right] \\ &\quad \times \sum_{i=1}^{k-k\beta_0} \frac{1}{P_1(m_{opt}, \beta_0 + \frac{i}{k}) + P_2(m_{opt}, \beta_0 + \frac{i}{k})}. \end{aligned} \tag{46}$$

$$\begin{aligned} O_{\text{IOFC}} &= k + \frac{kc}{2} + (m-1)\left[1 - \frac{c(1-\beta_0)}{2}\right] \\ &\quad \times \sum_{i=1}^{k-k\beta_0} \frac{1}{P_1(m_{opt}, \beta_0 + \frac{i}{k}) + P_2(m_{opt}, \beta_0 + \frac{i}{k})}. \end{aligned} \tag{47}$$

E. Analysis of Coding Efficiency

Definition 2: The ratio of the number of useful encoded packets N_{useful} to the total number of transmitted encoded

packets N_{total} is defined as the coding efficiency, which is expressed as follows:

$$R_{\text{ce}} = \frac{N_{\text{useful}}}{N_{\text{total}}}. \tag{48}$$

With the OFC and the IOFC, the useful encoded packets include the encoded packets with degree 1 or 2 in the build-up phase and the encoded packets in Case 1 or Case 2 in the completion phase. According to [23], the number of useful encoded packets in the OFC and the IOFC are given by formulas (49) and (50), respectively.

$$N_{\text{useful}}^{\text{OFC}} = \frac{kc}{2} + \frac{1}{\beta_0} + \left[1 - \frac{c(1-\beta_0)}{2}\right](k - k\beta_0). \tag{49}$$

$$N_{\text{useful}}^{\text{IOFC}} = \frac{k}{2} + \frac{kc}{4} + \frac{1}{\beta_0} + \left[\frac{1}{2} - \frac{c(1-\beta_0)}{4}\right](k - k\beta_0). \tag{50}$$

With the ROFC, all the transmitted packets in the completion phase are of either Case 1 type or Case 2 type; thus, the number of useful encoded packets is equal to the number of transmitted packets, and $N_{\text{useful}}^{\text{ROFC}}$ is given by

$$N_{\text{useful}}^{\text{ROFC}} = \frac{kc}{2} + \frac{1}{\beta_0} + k(1-\beta_0)\left[1 - \frac{c(1-\beta_0)}{2}\right]. \tag{51}$$

Compared with the ROFC, due to the limitation of feedback in the ROFC-LF, some useless encoded packets are transmitted, but the number of useful encoded packets is still $N_{\text{useful}}^{\text{ROFC}}$; therefore, $N_{\text{useful}}^{\text{ROFC - LF}}$ is given by

$$N_{\text{useful}}^{\text{ROFC - LF}} = \frac{kc}{2} + \frac{1}{\beta_0} + k(1-\beta_0)\left[1 - \frac{c(1-\beta_0)}{2}\right]. \tag{52}$$

According to formulas (35), (36), (37), (38), (49), (50), (51), and (52), the coding efficiencies of the four coding schemes are obtained, which are expressed as $R_{\text{ce}}^{\text{OFC}}$, $R_{\text{ce}}^{\text{IOFC}}$, $R_{\text{ce}}^{\text{ROFC}}$ and $R_{\text{ce}}^{\text{ROFC - LF}}$, and it is easy to obtain that $R_{\text{ce}}^{\text{OFC}} < 1$, $R_{\text{ce}}^{\text{IOFC}} < 1$, $R_{\text{ce}}^{\text{ROFC}} = 1$ and $R_{\text{ce}}^{\text{ROFC - LF}} \leq 1$.

Useful encoded packets result in decoding progress at the receiver. However, useless encoded packets are not helpful in decoding and consume extra energy and channel bandwidth. Thus, for UANs, the closer to 1 R_{ce} is, the better the performance is. In addition, feedback packets increase the end-to-end delay of UANs and decrease the channel efficiency. Therefore, a coding scheme with R_{ce} close to 1 and fewer feedback packets is desirable for UANs.

F. Analysis of Energy Consumption

In this section, the energy consumed by one-hop transmission in UANs is analyzed. The size of each encoded packet is set to L_{e} bits. The size of each ACK is set to L_{A} bits. The propagation distance is d meters, and the propagation speed is v m/s. The transmission rate is R bit/s. The transition time between the sending and receiving states of the acoustic modem is set to t_s seconds. The transmitting power and the receiving power of the underwater node are assumed to be P_{tx} and P_{rx} Watts, respectively. The total energy consumption E_{total} for transporting a packet one hop includes the energy consumption for processing data (i.e., basic energy consumption), the energy consumption for sending packets and receiving ACK (where ACK is the feedback packet) E_{send}, and the energy consumption for receiving packets and sending ACK, E_{rec}. E_{send} and E_{rec} are the energy consumptions for communication. In UANs, the basic energy consumption is much smaller than that for communication, so it can be ignored.

The energy consumption of the sender is the energy consumption of sending N_{e} encoded packets and receiving N_{A} ACK packets. E_{send} (units of Joules) is given by

$$E_{\text{send}} = P_{\text{tx}}T_{\text{e}} + P_{\text{rx}}T_{\text{A}}. \tag{53}$$

where T_{e} is the time for sending N_{e} encoded packets, so $T_{\text{e}} = N_{\text{e}}L_{\text{e}}/R$. T_{A} is the time for receiving N_{A} ACK packets, so $T_{\text{A}} = N_{\text{A}}L_{\text{A}}/R$.

The energy consumption of the receiver for receiving N_{e} encoded packets and sending N_{A} ACK packets, E_{rec} is given by

$$E_{\text{rec}} = P_{\text{rx}}T_{\text{e}} + P_{\text{tx}}T_{\text{A}}. \tag{54}$$

According to equations (53) and (54), the total energy consumption is

$$\begin{aligned} E_{\text{total}} &= (P_{\text{tx}} + P_{\text{rx}})T_{\text{e}} + (P_{\text{tx}} + P_{\text{rx}})T_{\text{A}} \\ &= (P_{\text{tx}} + P_{\text{rx}})\frac{L_{\text{e}}}{R}N_{\text{e}} + (P_{\text{tx}} + P_{\text{rx}})\frac{L_{\text{A}}}{R}N_{\text{A}}. \end{aligned} \tag{55}$$

According to the analysis of the codec and feedback in sections IV.A and IV.B, the energy consumption formulas of the OFC, IOFC, ROFC and ROFC-LF can be easily obtained.

V. Transport Mechanism

When a receiver needs to feed back an ACK, it switches to the sending state and transmits the feedback packet. If the feedback packet arrives at the sender in the sending state, collision and retransmission occur, which reduces channel utilization and increases latency and energy consumption. To overcome these problems, we propose a hop-by-hop transport mechanism based on the ROFC-LF for UANs, which is described below.

In the build-up phase, the sender first sends an encoded packet with degree 2, in which the immediate acknowledge bit is 1, and then switches to the receiving state to receive the ACK. After receiving an encoded packet in which the immediate acknowledge bit is 1, the receiver responds to the sender with an ACK packet including a 1-bit ready field and a k-bit decoding-state field. The value 1 in the ready field means that the receiver has received the first encoded packet and is ready to receive the subsequent packets. The decoding-state field is used to feed back to the sender the size of the largest component and the decoding state.

After sending $N_1 = kc/2 + \eta$ encoded packets with degree 2, the sender switches to the receiving state to wait for an ACK. If the value of the decoding-state field in the received ACK packet is neither all zeros nor all 1s, the sender switches to the sending state and continues to send $N_2 = kc/2(1 - D_1/k\beta_0)$ encoded packets with degree 2, then

switches to the receiving state for an ACK. This process continues until an ACK packet with the value of all 1s in the decoding-state field is received, which means the size of the largest component has reached $\beta_0 k$. Then, the sender sends $1/\beta_0 + \mu$ encoded packets with degree 1, which are used to decode the encoded packets in the largest component. According to the codec analysis in Section IV.A, the numbers N_1 and N_2 are set to $N_1 = kc/2 + \eta$ and $N_2 = kc/2(1 - D_1/k\beta_0)$. η is related to the number of original packets k. The η extra encoded packets with degree 2 ensure that the largest component can be determined rapidly. The μ encoded packets with degree 1 ensure that the largest component can be successfully decoded rapidly.

To facilitate recursive encoding, the original packets are classified into two sets: the set of recovered original packets $Y_i(|A|, SNs)$ and the set of unrecovered original packets $W_i(k - |A|, SNs)$. In the completion phase, the sender randomly encodes original packets from the set $W_i(k - |A|, SNs)$ with degree 1 or 2, and the receiver determines whether to send an ACK according to the threshold δ. The sender updates the two sets $Y_i(|A|, SNs)$ and $W_i(k - |A|, SNs)$ according to the field of the decoding state in the received ACK packet. This process continues until the ACK packet is received, which implies that the decoding-state field indicates that all the original packets have been recovered successfully.

VI. Performance Evaluation

In this section, the performance of the ROFC-LF is evaluated by simulation experiments and numerical analysis and is compared with the OFC, IOFC, and OFC-LF in [26] and the proposed ROFC. Although the probability of cycles and useless encoded packets is very small with the ROFC-LF, the limitation of the number of feedback packets and the small proportion of encoded packets of Case 1 type lead to some helpless encoded packets being generated. In the simulation, each group of experiments is tested 50 times, and the final result is obtained by averaging the 50 results and is presented in the respective figures. "Analysis" in the figures represents the theoretical analysis results, and "Simulation" represents the experimental simulation results.

According to [23], when $\beta_0 = 0.5$, the overhead is the lowest for the OFC and IOFC schemes. Therefore, β_0 is set to 0.5 in the simulation experiments. The numbers of encoded packets or feedback packets required to recover all the original packets with the ROFC-LF, ROFC, OFC and IOFC are shown in Figs. 6-8 based on the theoretical analysis and formulas (35)-(38) in section IV.

From Fig. 6, it can be seen that to recover the same number of original packets, the number of encoded packets required with the ROFC is the lowest among the three coding schemes (the ROFC, OFC and IOFC). This is because with the ROFC, the SNs of the recovered original packets are implied in the feedback packets, which is convenient for recursive encoding. With recursive encoding, each encoded packet is helpful for recovering the remaining original packets. Therefore, the ROFC decreases the number of encoded packets required for recovering a certain number of original packets.

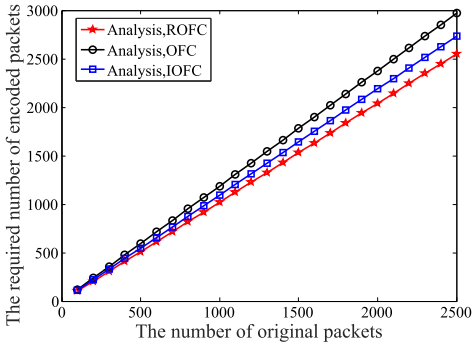

Fig. 6. The number of the original packets vs. the required number of the encoded packets.

TABLE III
The Variances of the Experimental Results

k	β_0	α	δ	variances
100	0.5	0.1	0.006	70
500	0.5	0.5	0	22
500	0.5	0.1	0.006	99.7
1000	0.5	0.1	0.006	158.2

Fig. 7(a) shows that the results of the theoretical analysis are consistent with those of the simulation experiments. For the ROFC, when $\alpha \geq 0.4$, the number of required encoded packets obtained through analysis is almost the same as that obtained through the simulation experiment. When $\alpha < 0.4$ (the encoded packets in Case 1 account for less than 40%), the number of encoded packets obtained through analysis is less than that obtained through the simulation experiment. Fig. 7(b) shows that with increasing α, the number of required feedback packets increases. In UANs, more feedback packets cause longer delay, more energy consumption, and lower channel efficiency. Considering the negative effect of too many feedback packets on UANs, the minimum value of α is desirable, i.e., $\alpha = 0.1$, which is consistent with the analysis result in section IV. Therefore, we set $\alpha = 0.1$ in the simulation experiments shown in Figs. 9-13.

The experiments are divided into four groups with four parameter settings. Each group was tested 50 times, so we obtained fifty numbers of encoded packets that were capable of recovering all original packets. The parameter settings and number variance of the encoded packets in each group are listed in TABLE III. According to Fig. 7(a), when $\beta_0 = 0.5$, $\alpha = 0.5$ and $\delta = 0$, the simulation results are consistent with the theoretical results. When $\alpha = 0.5$ and $\delta = 0$, there are few useless encoded packets, and the variance of the number of encoded packets used for recovering all original packets is minimal. However, when $\beta_0 = 0.5$, $\alpha = 0.1$, and $\delta = 0.006$, due to the limited feedback and reduced proportion of encoded packets in Case1, the useless encoded packets are transmitted, and the variance of this group experiment is maximal.

In Fig. 8, $\Delta\beta$ for the ROFC-LF is set to 0.006 according to the analysis of $\Delta\beta$ in section III. When $\alpha = 0.1$, both the numbers of encoded packets and the numbers of feedback packets required by the two encoding mechanisms are relatively low, which is the same in Fig. 7. Therefore, when $\alpha = 0.1$, the performance of the ROFC-LF mechanism is

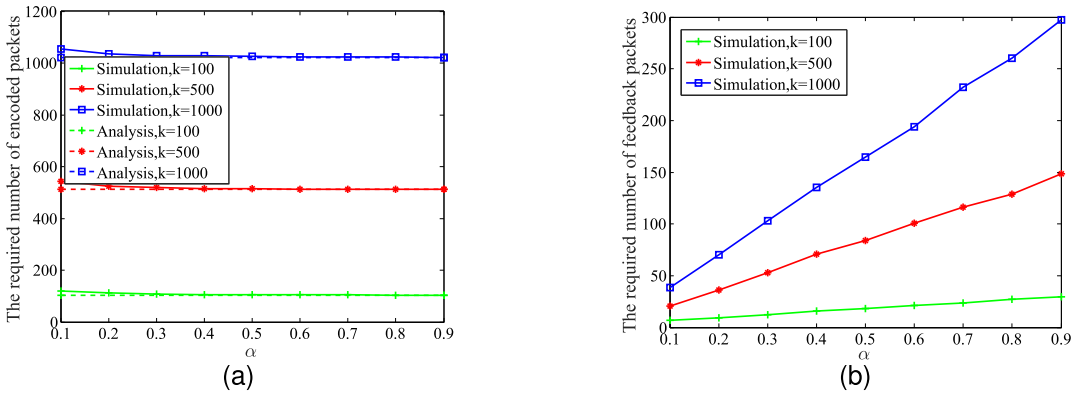

Fig. 7. shows the effects of α on the required numbers of encoded packets and feedback packets with the ROFC when $k = 100$, $k = 500$ and $k = 1000$. (a) The effect of α on the required number of encoded packets. (b) The effect of α on the required number of feedback packets.

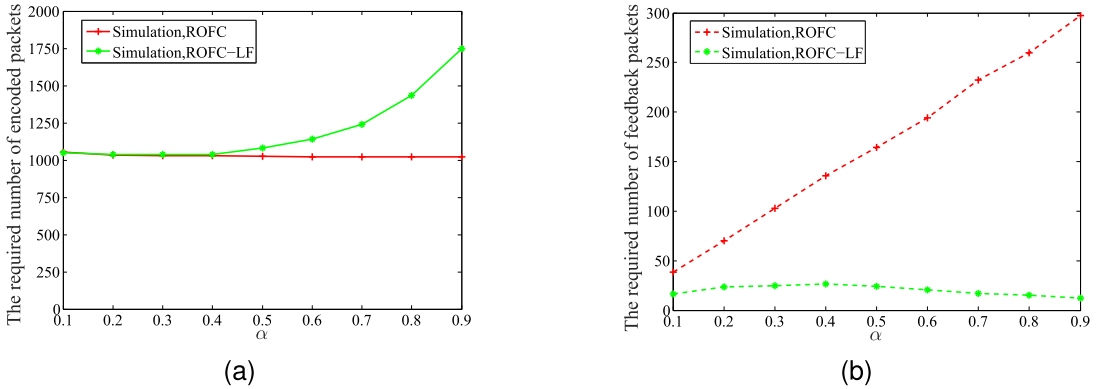

Fig. 8. shows the effect of α on the numbers of encoded packets and feedback packets for $k = 1000$ with the ROFC and ROFC-LF schemes.(a) The effect of α on the required number of encoded packets. (b) The effect of α on the required number of feedback packets.

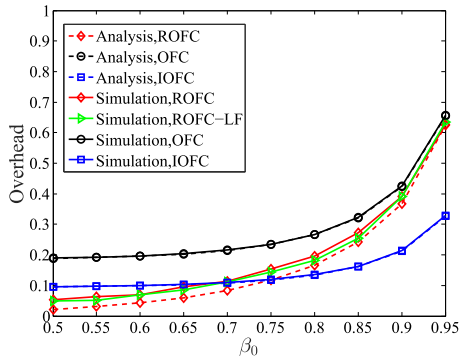

Fig. 9. The effect of β_0 on the overhead.

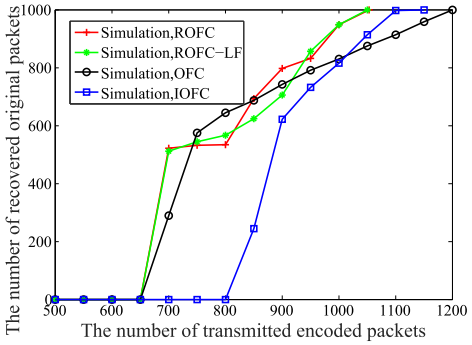

Fig. 10. The number of recovered original packets vs. the number of transmitted encoded packets.

also the best. Consistent with the theoretical analysis, when $\alpha = 0.1$, the numbers of encoded packets required by the two encoding mechanisms are almost the same, but the number of feedback packets required by the ROFC-LF is much smaller than that of the ROFC. The limited feedback is preferable for UANs. Therefore, we set $\alpha = 0.1$ in the experiments shown in Figs. 9-13.

Fig. 9 shows the effect of β_0 on the overhead for $k = 1000$. For comparison with the OFC and IOFC, we set $k = 1000$ and $\beta_0 \in [0.5, 0.95]$ according to [23]. Fig. 9 shows that the overhead increases with β_0 with any of the four coding schemes. The simulation results with the OFC and IOFC are consistent with the respective theoretical results in [23]. Due to the restricted feedback, the overhead with the ROFC-LF obtained from the simulation results is slightly larger than that with the ROFC from the theoretical analysis, which accords with the theoretical analysis and formulas (40)-(43) in section IV. Since α is set to 0.1 in the simulation experiment, the overhead with the ROFC obtained through simulation is slightly higher than that obtained through theoretical analysis, which is consistent with the results in Fig. 7. When β_0 varies from 0.5 to 0.95, the overheads with the ROFC and ROFC-LF are lower than those with the OFC. When $\beta_0 < 0.7$, the overheads with the ROFC-LF and ROFC are smaller than those with the IOFC. As seen in Fig. 9, when $\beta_0 = 0.5$, the overheads of all the schemes are the lowest. Consequently, β_0 is set to 0.5 in Fig. 10, Fig. 11 and Fig. 13.

Fig. 10 shows the effects of the numbers of transmitted encoded packets on the numbers of recovered original packets

TABLE IV
COMPUTATIONAL COMPLEXITIES

Schemes	Computational complexity
OFC	2(550($m_{\text{opt}}-1$)+650)>4348
IOFC	2(350($m_{\text{opt}}-1$)+800)>3540
ROFC	2028
ROFC-LF	2022

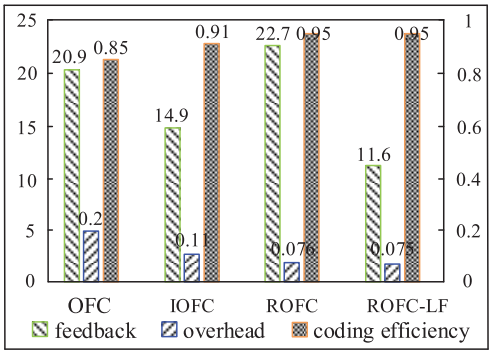

Fig. 11. Comparison of the overhead, coding efficiency and number of feedback packets for $k = 512$.

for $k = 1000$ and $\beta_0 = 0.5$ according to [23]. From Fig. 10, it can be seen that either the ROFC or ROFC-LF has obvious advantages in decoding speed. The number of encoded packets needed by the ROFC or ROFC-LF is less than that needed by the OFC and IOFC to recover the same number of original packets. A total of 650 encoded packets with degree 2 are required in the build-up phase with the OFC, ROFC or ROFC-LF, while 800 encoded packets are required with the IOFC. In the completion phase, for $\alpha = 0.1$, to recover all the original packets, 364 encoded packets with degree 2 are required with the ROFC, while 361 encoded packets with degree 2 are required with the ROFC-LF. In comparison, with either the OFC or IOFC, the packets are encoded with the optimal degree m_{opt}, which is fed back by the receiver, and m_{opt} changes dynamically with the progress of decoding. With the OFC, 550 encoded packets with m_{opt} are required, while with the IOFC, 350 encoded packets with m_{opt} are required. In summary, according to the above analysis and formulas (44)-(47) in section IV, the computational complexities of the four codings are as shown in TABLE IV.

For the OFC or IOFC, the optimal degree m_{opt} changes dynamically in the completion phase. The lower bounds of the numbers of XOR operations with the OFC and IOFC as well as the approximate numbers with the ROFC and ROFC-LF are shown in TABLE IV. To calculate a more accurate lower bound of XOR operations with the OFC or IOFC, the average degree m is calculated according to TABLE II, where $\hat{m} \leq \sum_{m_{\text{opt}}=1}^{30} m_{\text{opt}} \Delta \beta_s$. In the OFC or IOFC, there may be some encoded packets with a larger degree than 30, so the number of XOR operations with the OFC or IOFC increases significantly with the degree m_{opt}. Therefore, the number of XOR operations with either the ROFC-LF or ROFC is smaller than that with the OFC or IOFC.

Fig. 11 gives a performance comparison in terms of the overhead, coding efficiency and number of feedback packets

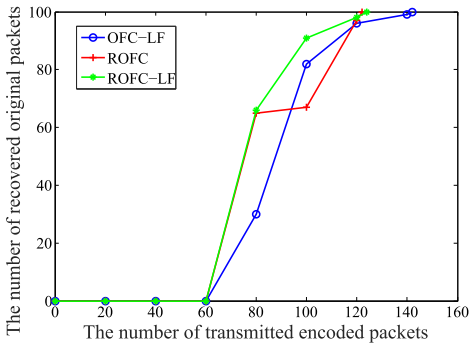

Fig. 12. The number of recovered original packets vs. the number of transmitted encoded packets.

for $k = 512$. For comparison with the OFC and IOFC, we set $k = 512$ and $\beta_0 = 0.5$ according to [23]. From Fig. 11, it can be seen that the overhead and the number of feedback packets of the ROFC-LF are the lowest among the four coding schemes. The coding efficiency of the ROFC-LF and ROFC is higher than that of the OFC and IOFC. In summary, both proposed codings, the ROFC and ROFC-LF, outperform the OFC and IOFC in terms of overhead, coding efficiency and the number of required feedback packets, and they are more suitable for UANs.

To further demonstrate the advantages of the ROFC-LF, we compare it with the ROFC and OFC-LF proposed in [26]. We set $k = 100$ and $\beta_0 = 0.65$ according to [26]. The results show that the ROFC-LF has better intermediate decoding performance and requires fewer encoded packets. To recover 100 original packets, the OFC-LF, ROFC and ROFC-LF need to send 3, 7 and 6 feedback packets, respectively. Therefore, the OFC-LF requires fewer feedback packets but more encoded packets. However, the ROFC-LF performs well in both respects, so the ROFC-LF is preferable for UANs with constrained resources.

In the legend of Fig. 13, ROFC-LF-0.006 means that the threshold δ of the ROFC-LF is set to 0.006, and so on. Fig. 13 shows that when k is fixed, the numbers of encoded packets required by ROFC-LF-0.006 and ROFC-LF-0.01 are almost the same as those required by the ROFC, while the numbers of feedback packets are much less than those of the ROFC. When δ is set to a larger value (for example, $\delta = 0.02$ or $\delta = 0.1$), more encoded packets are required and fewer feedback packets are sent. When $k > 1000$, the number of feedback packets required remains largely unchanged for the same δ. When $k < 1000$, the average number of encoded packets required by the ROFC-LF is almost the same for $\delta = 0.006$, $\delta = 0.01$ and $\delta = 0.02$. Therefore, when $k < 1000$, to decrease the number of feedback packets and improve the channel efficiency, δ is set to 0.02 in UANs.

To evaluate the energy consumption, we set the following parameters as in [19] and [20]: $P_{\text{tx}} = 20$ W, $P_{\text{rx}} = 1$ W, $L_{\text{e}} = 268$ bytes, $R = 2000$ bps. When k is 1000, 512 and 100, L_{A} is set to 129 bytes, 68 bytes and 17 bytes in the ROFC and ROFC-LF, respectively. L_{A} with LT code is set to 4 bytes regardless of the value of k. When k is 512, L_{A} is set to 6 bytes in both the OFC and IOFC schemes. When k is 100, L_{A} is set to 5 bytes in the OFC-LF scheme.

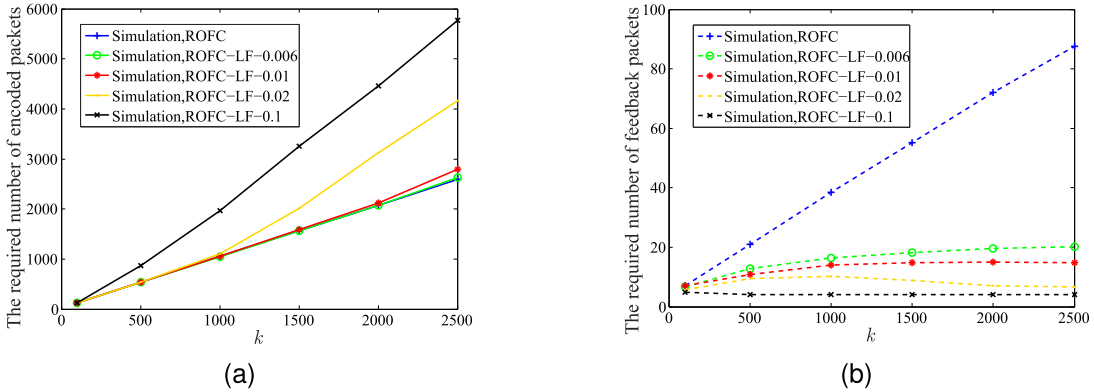

Fig. 13. shows the effects of k and δ on the numbers of required encoded packets and feedback packets. (a) The effect of k and δ on the required number of encoded packets. (b) The effect of k and δ on the required number of feedback packets.

TABLE V
ENERGY CONSUMPTION FOR $k = 1000$ AND $\beta_0 = 0.5$

schemes	N_{e}	N_{A}	E_{total}
LT	1400	1	31517.1 J
ROFC	1054.1	38.4	24146.0 J
ROFC-LF	1048.4	16.5	23780.4 J

TABLE VI
ENERGY CONSUMPTION FOR $k = 100$ AND $\beta_0 = 0.65$

schemes	N_{e}	N_{A}	E_{total}
OFC-LF	142	3	3198.0 J
ROFC	122	7.1	2756.6 J
ROFC-LF	124	5.7	2799.6 J

TABLE VII
ENERGY CONSUMPTION FOR $k = 512$ AND $\beta_0 = 0.5$

schemes	N_{e}	N_{A}	E_{total}
OFC	614.4	20.9	13841.9 J
IOFC	568.3	14.9	12801.1 J
ROFC	550.9	22.7	12531.5 J
ROFC-LF	550.4	11.6	12456.9 J

Since the parameter settings are different in different works on the LT, OFC, IOFC and OFC-LF schemes, to compare the performance of the four codings, we set three group parameters and obtain three results of energy consumption. TABLE V lists the energy consumptions of the LT code, ROFC and ROFC-LF for $k = 1000$ and $\beta_0 = 0.5$. TABLE VI lists the energy consumptions of the OFC-LF, ROFC and ROFC-LF for k= 100 and $\beta_0 = 0.65$. TABLE VII lists the energy consumptions of the ROFC, ROFC-LF, IOFC and OFC for $k = 512$ and $\beta_0 = 0.5$. The proposed ROFC and ROFC-LF outperform the LT code, OFC-LF, IOFC and OFC in terms of energy consumption.

VII. CONCLUSION

This paper proposes a recursive online fountain code with limited feedback (ROFC-LF) for UANs. In the ROFC-LF, the original packets are classified into two sets, the recovered set and unrecovered set. The encoded packets are generated by XORing the original packets in the unrecovered set, so each encoded packet is helpful for decoding. To reduce the size of the feedback packets, the states and the SNs of the original packets are encoded and sent to the sender. Furthermore, the number of feedback packets is restricted through a decoding progress threshold. Theoretical analyses and simulation experiments show that compared with the traditional OFC, the proposed ROFC-LF improves the coding efficiency by 10%, while the number of required encoded packets (overhead), the number of feedback packets, and the computational complexity are reduced by at least 12%, 44%, and 53%, respectively. Compared with the IOFC, the ROFC-LF improves the coding efficiency by 4%, while the number of required encoded packets (overhead), feedback packets, and the computational complexity are reduced by at least 3%, 22%, and 42%, respectively. With the OFC-LF, the number of feedback packets is limited, but a large number of useless encoded packets are generated and transmitted. In contrast, the ROFC-LF performs well in both respects. With the ROFC-LF, more original packets are recovered when receiving the same number of encoded packets as in the OFC, IOFC and OFC-LF. The optimum values of the parameters α and δ in the ROFC-LF for UANs can be obtained through a large number of simulation experiments and analyses. Both theoretical and simulation results show that the ROFC-LF outperforms the OFC, IOFC, OFC-LF and even ROFC in terms of overhead, number of feedback packets, computational complexity, coding efficiency and energy consumption.

REFERENCES

[1] L. Yan, X. Ma, X. Li, and J. Lu, "Shot interference detection and mitigation for underwater acoustic communication systems," *IEEE Trans. Commun.*, vol. 69, no. 5, pp. 3274–3285, May 2021.
[2] L. Wang, Y. Yang, and X. Liu, "A direct position determination approach for underwater acoustic sensor networks," *IEEE Trans. Veh. Technol.*, vol. 69, no. 11, pp. 13033–13044, Nov. 2020.
[3] S. Jiang, "On reliable data transfer in underwater acoustic networks: A survey from networking perspective," *IEEE Commun. Surveys Tuts.*, vol. 20, no. 2, pp. 1036–1055, 2nd Quart., 2018.
[4] A. Lee-Leon, C. Yuen, and D. Herremans, "Underwater acoustic communication receiver using deep belief network," *IEEE Trans. Commun.*, vol. 69, no. 6, pp. 3698–3708, Jun. 2021.
[5] Y. Zhang, Z. Zhang, L. Chen, and X. Wang, "Reinforcement learning-based opportunistic routing protocol for underwater acoustic sensor networks," *IEEE Trans. Veh. Technol.*, vol. 70, no. 3, pp. 2756–2770, Mar. 2021.
[6] R. W. L. Coutinho and A. Boukerche, "OMUS: Efficient opportunistic routing in multi-modal underwater sensor networks," *IEEE Trans. Wireless Commun.*, vol. 20, no. 9, pp. 5642–5655, Sep. 2021.

[7] X. Du, K. Li, X. Liu, and Y. Su, "RLT code based handshake-free reliable MAC protocol for underwater sensor networks," *J. Sensors*, vol. 2016, pp. 1–11, Feb. 2016.

[8] W. Raza, X. Ma, A. Ali, Z. A. Shah, and G. Mehdi, "An implementation of partial transmit sequences to design energy efficient underwater acoustic OFDM communication system," *Int. J. Comput. Sci. Inf. Secur.*, vol. 18, no. 4, pp. 1–8, Apr. 2020.

[9] F. A. de Souza, B. S. Chang, G. Brante, R. D. Souza, M. E. Pellenz, and F. Rosas, "Optimizing the number of hops and retransmissions for energy efficient multi-hop underwater acoustic communications," *IEEE Sensors J.*, vol. 16, no. 10, pp. 3927–3938, May 2016.

[10] J. W. Byers, M. Luby, M. Mitzenmacher, and A. Rege, "A digital fountain approach to reliable distribution of bulk data," *SIGCOMM Comput. Commun. Rev.*, vol. 28, no. 4, pp. 56–67, Oct. 1998.

[11] M. Luby, "LT codes," in *Proc. 43rd Annu. IEEE Symp. Found. Comput. Sci.*, Nov. 2002, pp. 271–280.

[12] A. Shokrollahi, "Raptor codes," *IEEE Trans. Inf. Theory*, vol. 52, no. 6, pp. 2551–2567, Jun. 2006.

[13] W. Yao, B. Yi, T. Huang, and W. Li, "Poisson robust soliton distribution for LT codes," *IEEE Commun. Lett.*, vol. 20, no. 8, pp. 1499–1502, Aug. 2016.

[14] A. Hagedorn, S. Agarwal, D. Starobinski, and A. Trachtenberg, "Rate less coding with feedback," in *Proc. INFOCOM*, Apr. 2009, pp. 1791–1799.

[15] A. Yazdanialahabadi and M. Ardakani, "A distributed low-complexity coding solution for large-scale distributed FFT," *IEEE Trans. Commun.*, vol. 68, no. 11, pp. 6617–6628, Nov. 2020.

[16] T. Okpotse and S. Yousefi, "Systematic fountain codes for massive storage using the truncated Poisson distribution," *IEEE Trans. Commun.*, vol. 67, no. 2, pp. 943–954, Feb. 2019.

[17] L. Sun, D. Huang, and A. L. Swindlehurst, "Fountain-coding aided secure transmission with delay and content awareness," *IEEE Trans. Veh. Technol.*, vol. 69, no. 7, pp. 7992–7997, Jul. 2020.

[18] H. U. Yildiz, "Maximization of underwater sensor networks lifetime via fountain codes," *IEEE Trans. Ind. Informat.*, vol. 15, no. 8, pp. 4602–4613, Aug. 2019.

[19] Y. Song, "Underwater acoustic sensor networks with cost efficiency for internet of underwater things," *IEEE Trans. Ind. Electron.*, vol. 68, no. 2, pp. 1707–1716, Feb. 2021.

[20] D. H. Simao, B. S. Chang, G. Brante, M. E. Pellenz, and R. D. Souza, "Energy efficiency of multi-hop underwater acoustic networks using fountain codes," *IEEE Access*, vol. 8, pp. 23110–23119, 2020.

[21] A. Kamra, V. Misra, J. Feldman, and D. Rubenstein, "Growth codes: Maximizing sensor network data persistence," *ACM SIGCOMM Comput. Commun. Rev.*, vol. 36, no. 4, pp. 255–266, Oct. 2006.

[22] Y. Cassuto and A. Shokrollahi, "Online fountain codes with low overhead," *IEEE Trans. Inf. Theory*, vol. 61, no. 6, pp. 3137–3149, Jun. 2015.

[23] J. Huang, Z. Fei, C. Cao, M. Xiao, and D. Jia, "Performance analysis and improvement of online fountain codes," *IEEE Trans. Commun.*, vol. 66, no. 12, pp. 5916–5926, Dec. 2018.

[24] T. Huang and B. Yi, "Improved online fountain codes based on shaping for left degree distribution," *AEU Int. J. Electron. Commun.*, vol. 79, pp. 9–15, Sep. 2017.

[25] Y. Zhao, Y. Zhang, F. C. M. Lau, H. Yu, and Z. Zhu, "Improved online fountain codes," *IET Commun.*, vol. 12, no. 18, pp. 2297–2304, Nov. 2018.

[26] P. Cai, Y. Zhang, Y. Wu, X. Chang, and C. Pan, "Feedback strategies for online fountain codes with limited feedback," *IEEE Commun. Lett.*, vol. 24, no. 9, pp. 1870–1874, Sep. 2020.

[27] J. Huang, Z. Fei, C. Cao, and M. Xiao, "Design and analysis of online fountain codes for intermediate performance," *IEEE Trans. Commun.*, vol. 68, no. 9, pp. 5313–5325, Sep. 2020.

[28] P. Shi, Z. Wang, D. Li, and W. Xiang, "Zigzag decodable online fountain codes with high intermediate symbol recovery rates," *IEEE Trans. Commun.*, vol. 68, no. 11, pp. 6629–6641, Nov. 2020.

[29] J. Huang, Z. Fei, C. Cao, M. Xiao, and X. Xie, "Reliable broadcast based on online fountain codes," *IEEE Commun. Lett.*, vol. 25, no. 2, pp. 369–373, Feb. 2021.

[30] P. Erdős and A. Rényi, "On the evolution of random graphs," *Pub. Math. Inst. Hungarian Acad. Sci.*, vol. 5, pp. 17–61, Jan. 1960.

[31] N. Alon and J. Spencer, *The Probabilistic Method*. Hoboken, NJ, USA: Wiley, 2000.

Xiuxiu Liu received the B.E. and M.E. degrees from Qinghai Normal University, Xining, China, in 2013 and 2016, respectively, where she is currently pursuing the Ph.D. degree. She is also a Lecturer with Qinghai Normal University. Her research interest includes underwater acoustic networks.

Xiujuan Du received the M.E. degree from Lanzhou University and the Ph.D. degree Tianjin University. She is currently a Professor with the Provincial Key Laboratory of the Internet of Things, Qinghai Normal University, Xining, China. Her research interests include network and information security, mobile *ad-hoc* networks, and underwater sensor networks. She received the New Century Excellent Talent from the Education Ministry of China in 2011.

Jiliang Zhang (Senior Member, IEEE) received the B.E., M.E., and Ph.D. degrees from the Harbin Institute of Technology, Harbin, China, in 2007, 2009, and 2014, respectively.

He was a Post-Doctoral Fellow with the Shenzhen Graduate School, Harbin Institute of Technology, from 2014 to 2016, an Associate Professor with the School of Information Science and Engineering, Lanzhou University, from 2017 to 2019, a Researcher with the Department of Electrical Engineering, Chalmers University of Technology, Gothenburg, Sweden, from 2017 to 2018, and a Marie Curie Research Fellow with the Department of Electronic and Electrical Engineering, The University of Sheffield, Sheffield, U.K., from 2019 to 2021, where he is currently a KTP Associate with the Department of Electronic and Electrical Engineering. His current research interests include wireless channel modeling, modulation systems, relay systems, vehicular communications, ultra-dense small cell networks, and smart environment modeling. He has been an Academic Editor for *Wireless Communications and Mobile Computing*, since 2019. He received the IEEE Wireless Communications Letters Exemplary Reviewer Award in 2021.

Duoliang Han received the B.E. and M.E. degrees from Qinghai Normal University, Xining, China, in 2017 and 2020, respectively, where he is currently pursuing the Ph.D. degree. His research interests include protocol design and optimization.

Long Jin (Senior Member, IEEE) received the B.E. degree in automation and the Ph.D. degree in information and communication engineering from Sun Yat-sen University, Guangzhou, China, in 2011 and 2016, respectively.

He received postdoctoral training with the Department of Computing, The Hong Kong Polytechnic University, Hong Kong, from 2016 to 2017. In 2017, he joined the School of Information Science and Engineering, Lanzhou University, as a Professor of computer science and engineering. He received the Excellent Doctoral Dissertation Award of Chinese Association for Artificial Intelligence (CAAI). His current research interests include neural networks, robotics, optimization, and intelligent computing.